Solid Freeform Fabrication 2018: Proceedings of the 29th Annual International Solid Freeform Fabrication Symposium – An Additive Manufacturing Conference
Reviewed Paper

Topology Optimisation of Additively Manufactured Lattice beams for three-point bending test

R. Rashid[a,b *], S.H. Masood[a], D. Ruan[a], S. Palanisamy[a,b], X. Huang[a], R.A. Rahman Rashid[a,b]
[a] *Faculty of Science, Engineering and Technology, Swinburne University of Technology, Victoria 3122, Australia*
[b] *Defence Materials Technology Centre, Victoria 3122, Australia*

Abstract

The ability of additive manufacturing to develop parts with complex shapes has increased the bandwidth of product design. This has facilitated the use of Topology Optimisation (TO) techniques to optimise the distribution of material throughout the part, thereby obtaining minimum weight without compromising the mechanical performance of the component. In this study the Bi-directional Evolutionary Structural Optimisation (BESO) algorithm was used to generate topologically optimised lattice unit cells. A simple bending beam with 50% reduced volume was printed in two different unit cell arrangements using Selective Laser Melting (SLM) process. Prior to printing, the density of SLM-printed AlSi12 samples was enhanced by using appropriate scanning strategy. The flexural properties of these topology optimised beams were compared with the solid beam. The topologically optimised beams absorbed about seven times more energy per unit volume till the displacement of maximum bending load when compared with the solid beam at the same displacement.

Keywords: BESO method, Selective laser melting (SLM), scanning strategy, flexural testing, energy absorption

Introduction

Manufacturing industries, like automobile and aerospace, are ever evolving in different technologies to improve component performance. One of the most desirable result for these industries is to reduce component weight by significant proportions. A prospective direction of reducing weight of any component is during its design phase. Topology Optimisation (TO) is a design solution which mathematically solves for optimal material distribution within the required design domain under a set of constraints. Application of TO for structural components would significantly lower the part cost. There are many topology optimisation approaches like homogenization method, Solid Isotropic Material with Penalization (SIMP), level-set method and Bi-directional Evolutionary Structural Optimisation (BESO), which have been widely discussed [1]. Due to their simplicity, SIMP and BESO methods are popular with regards to generating design suitable for practical applications [2].

In the case of structural optimisation, SIMP method considers element density as a variable and assigns relative densities to each element based on the stiffness values [3]. The design solution of this approach leads to elements with intermediate relative densities between

* Corresponding author at: Faculty of Science, Engineering and Technology, Swinburne University of Technology, Victoria 3122, Australia.
Email address: rrashid@swin.edu.au (R. Rashid)

0 and 1, which are difficult to manufacture without converting the intermediate density regions into solid regions. This approach has been embedded in the commercial software like TOSCA for ABAQUS [4], GTAM for ANSYS [5] and Inspire for Altair Hyperworks [6]. Most commercial software use iso-surfacing techniques to convert the intermediate density elements (having relative densities between 0 and 1) into solid elements (relative density of 1). The conversion of elements with intermediate relative densities into solid elements would slightly increase the volume of the material in a topology optimised design. BESO method considers elemental densities as design variables for structural optimisation but only assigns elemental densities with discrete values, 0 or 1 [7]. As a result, the design solution obtained consists of void or solid elements, which could be easily manufactured with the help of Additive Manufacturing (AM) techniques.

Lattice structures are an ideal weight reducing solution which have been widely studied. Structural members consisting of repetitive lattice units have found to have better structural properties [8]. Incorporating design solution with lattice units would find application in fields like biomedical, automotive and aerospace industries [9, 10]. Also, there is a need to incorporate lattice units which are optimised to undertake loads pertaining to specific design problems. Moreover, there are commercial softwares like nTopology and Autodesk Netfabb that have successfully incorporated lattice design optimisation.

Topology optimised complex designs are successfully manufactured using plastic 3D printing and have performed as per design requirements [11-13]. Most studies have been directed towards manufacturing TO design products with AM processes like FDM and SLS. Very limited studies have been undertaken to apply methods to couple TO designs with metal additive technique like Selective Laser Melting (SLM) [14]. SLM is a metal powder-bed additive manufacturing technique, where the powder is melted with the help of laser source and is solidified quickly in an inert atmosphere. With precise control over the melting of the metal powder, this process creates part with high dimensional accuracy. However, the process is complex with several processing parameters affecting the relative density of the final part [15, Rashid, 2017 #153].

The objective of this study is to topologically optimise a simple beam for three point bend testing using lattice units and subsequently compare the flexural properties of topologically optimised beams with the solid beam. A modified BESO topology optimisation algorithm was used to generate two repetitive lattice units within the design region of the beam. The solid and topology optimised beams were printed using the SLM process with the machine specified processing parameters.

BESO Topology Optimised Lattice Units

A case study of a simple bending beam was studied, which could be extended to complex designs in later studies. A beam simply supported between a span of 70 mm, having a total length of 90 mm and a square cross section of 22.5 mm side, with a mid-point load was considered for topology optimisation. The beam dimensions and span length were selected based on published work by Rahman Rashid et. al. [16]. The considered condition for topology optimisation of the beam was to maximise stiffness of the beam with a 50% reduction in

volume. The design and non-design region for the beam is shown in Figure 1 (a). When the structural BESO algorithm [17] is applied to the non-design region, a design solution is obtained as shown in Figure 1 (b).

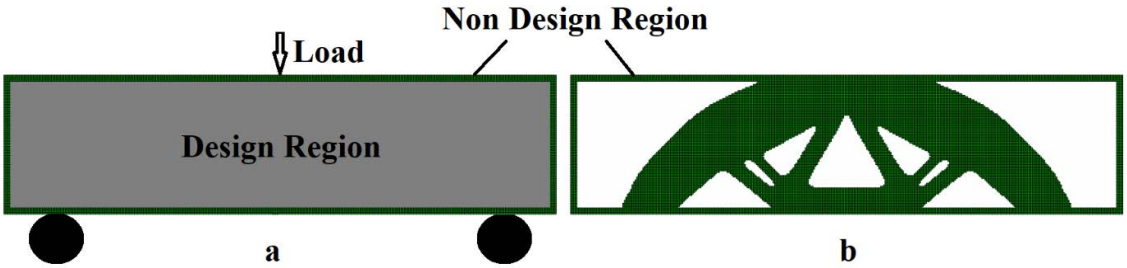

Figure 1. a) Solid beam (not topologically optimised); b) topology optimised beam without periodic constraints.

Topology optimisation could be used for this problem to generate homogeneous, symmetric or periodic material distributed designs with the help of optimised lattice units. Huang and Xie [18] reported that a modified BESO algorithm could be used to obtain unique topology optimised lattice units. The algorithm divides the design region into A×B lattice units, with A as number of lattice units in the X-direction and B as number of lattice units in Y as direction. The number of lattice units along the X and Y direction are selected by the designer. As an illustration, the design region shown in Figure 2 is divided into lattice units with 4 and 3 lattice units along X and Y direction, respectively. Therefore, the algorithm allows designers to select different periodic lattice units within the design region leading to unique designs.

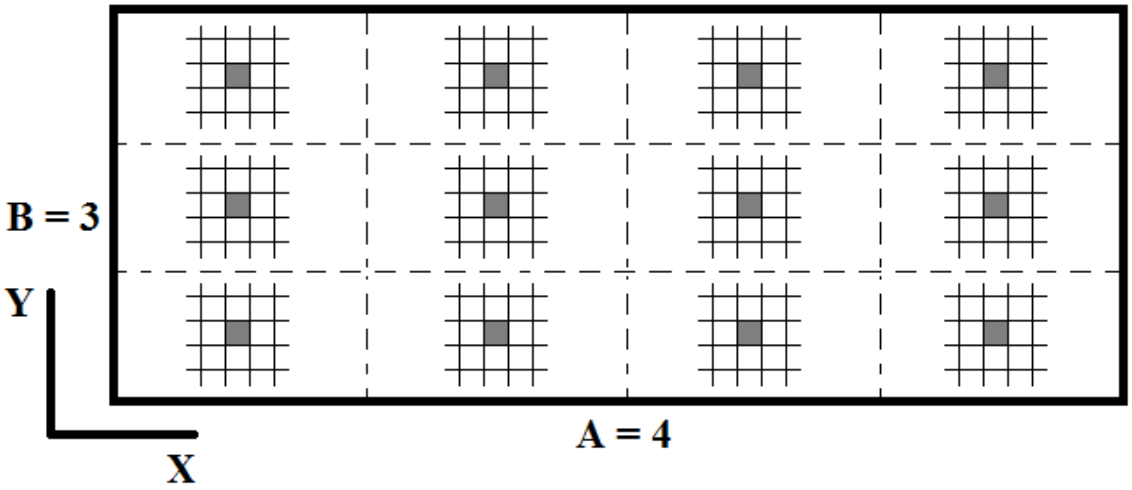

Figure 2. Design space divided into 4×3 lattice units, with grey region representing the elements which are linked to each other.

The conventional BESO method allows the addition or removal of elements from the entire design space based on their stiffness values. On the other hand, in this algorithm, the elements are added or removed from each lattice unit design region simultaneously. For example, the elements in grey colour, as shown in Figure 2, are linked to each other due to their similar location within the lattice units. Removal (or addition) of one such element in one lattice unit based on its stiffness value, would correspond to removal (or addition) of similarly located

elements in other lattice units. This leads to same lattice unit design within the design region. The algorithm could also be used to vary the design of the lattice units by controlling the number of units along the X and Y axes directions.

Based on this algorithm (explained in detail in [18]), an ABAQUS subroutine was developed to obtain topologically optimised beam with lattice units. A 2D beam with boundary conditions shown in Figure 1 (a) was considered for implementation of the algorithm in order to significantly reduce computation costs. The beam material considered for optimisation was isotropic in nature with Young's Modulus of 1GPa and Poisson's ratio of 0.33 as per the algorithm developed by [18]. The optimisation was done to minimise stiffness of the beam while reducing the volume of the beam to 50% while having periodic lattice units within the design region.

Two different variations of the optimised lattice units were considered for this study such that the design space was divided into 8×3 and 12×3 topology optimised lattice units. Specifically, the two design solutions had eight and twelve lattice units, respectively, along the length of the beam and three lattice unit along the height of the beam as shown in Figure 3 (a) and (b). Due to the removal/addition of elements in the optimised lattice units, the boundaries tend to have jagged boundaries as shown in Figure 4 (a) which are prominent in topology optimised design solutions. Therefore, a further boundary smoothening program (code presented in [19]) was applied to the optimised lattice unit design to obtain smooth boundaries, as shown in Figure 4 (b). The BESO lattice unit beam designs were too complex for fabrication using conventional machining. Hence, the beams were manufactured using Selective Laser Melting (SLM) additive manufacturing process.

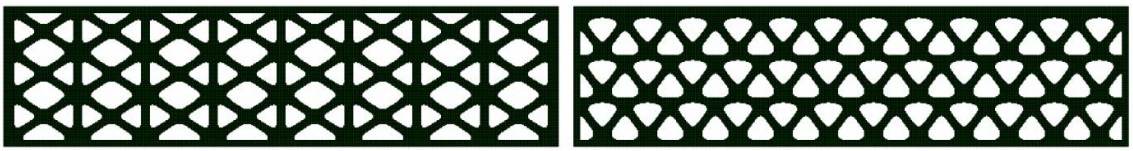

a b

Figure 3. a) 8×3 periodic lattice topology optimisation design; b) 12×3 periodic lattice topology optimisation design.

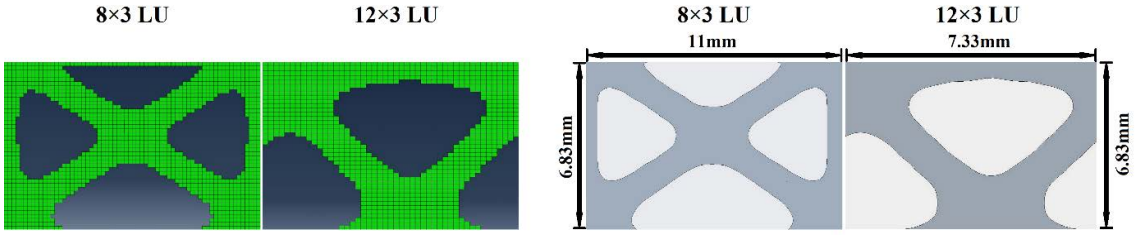

a b

Figure 4. a) Optimised lattice units with jagged boundaries; b) optimised lattice units post boundary smoothening process (LU – lattice unit).

SLM Process Parameters

The solid beam (shown in Figure 1 (a)) and BESO optimised lattice unit beams (shown in Figure 3 (a) and (b)) were printed using 3D Systems ProX 200 SLM machine. The samples

were printed using pre-alloyed AlSi12 powder which was acquired from 3D Systems. The obtained powder was then sieved to less than 45 µm. The powder particles were found to be pre-dominantly spherical in shape, which enhances the compactness of the powder layer for high density SLM parts. The samples were printed using machine specified process parameters presented in Table 1. The machine specified scanning strategy, referred as Scan H, was explained in detail elsewhere [20].

Table 1.SLM process parameters used to build AlSi12 samples

Laser Power (W)	Scan speed (mm/s)	Layer thickness (µm)	Hatch distance (µm)	Defocus Distance (mm)	Scanning Strategy
285	2500	40	100	-4	Scan H

In order to ascertain the relative density of the samples, analysis of the optical images were carried out. The microscopic analysis of SLM-printed samples was found to determine relative density with acceptable accuracy when compared to density measurement using X-Ray CT scan method [21, Rashid, 2017 #158]. The sample with square cross-section of 15mm edge and build height of 5mm was cut from substrate plate, mounted in epoxy resin and polished to observe under the optical microscope. The relative density was measured using Olympus Stream Motion software from optical microscope images of the polished surfaces as shown in Figure 5. It was found that the average relative density of the SLM-printed sample measured at three random surfaces along the build direction was 97.3 ± 1.0 %.

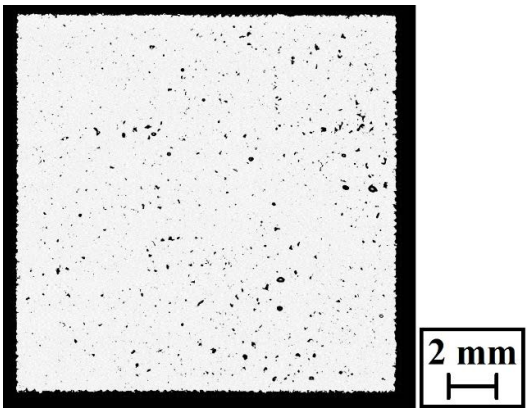

Figure 5. Macroscopic image of sample taken using optical microscope to measure relative density.

Using the SLM processing parameters mentioned in Table 1, the solid beam and 8×3 and 12×3 topology optimised lattice unit beams were printed in three separate batches. The SLM-printed samples were built with solid support structures of 3mm, making the entire build height of samples as 25.5mm. Subsequently, the SLM-printed beams were cut off the substrate and machined to a height of 22.5 mm. Figure 6 shows five samples each of the two topology optimised lattice units. Furthermore, prior to cutting the samples off the substrate plate, stresses in the SLM built samples were minimised by applying stress relief heat treatment.

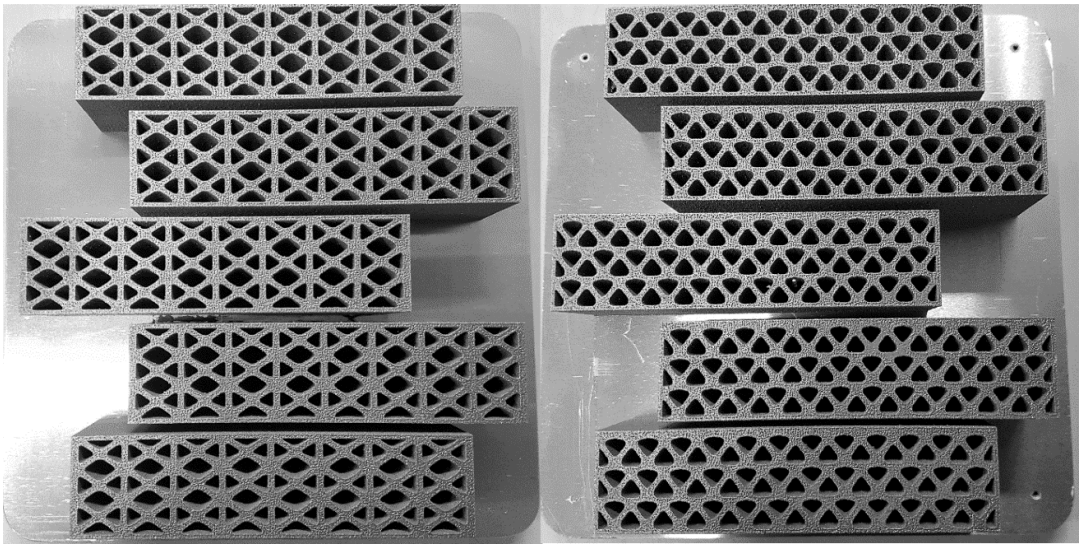

Figure 6. AlSi12 SLM-printed 8×3 lattice unit beams (left) and 12×3 lattice unit beams (right).

Flexural Bending Test

The bending tests were carried out on the MTS 50 kN machine with the test setup as shown in Figure 7. A quasi-static velocity of 3.33 mm/s was arbitrarily used in the bending tests. The force values were recorded with the help of the machine dynamometer and the deflection at the centre of the beam was recorded with the help of laser video extensometer. The span between the two circular rollers was set to 70 mm.

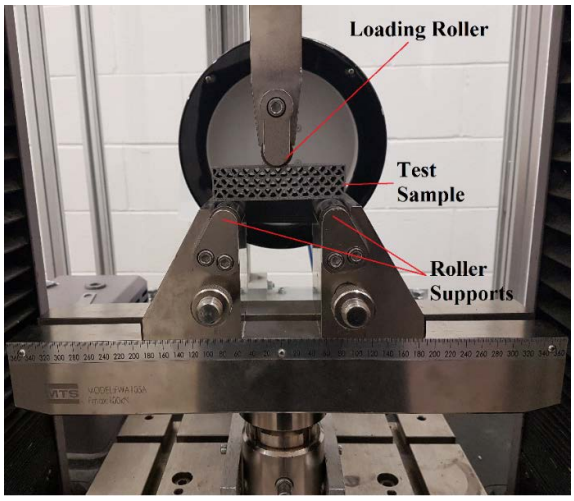

Figure 7. Bending test setup.

The experimental results were analysed and the graph between force and displacement was plotted as shown in Figure 8. The average maximum bending load, average deflection of the beam at maximum load and average deflection of the beam at complete failure[1] of three

[1] 'Complete failure' was considered to have been achieved when the load bearing capacity of the test specimen was reduced to 0.

samples each of solid, 8×3 and 12×3 beams are tabulated in Table 2. All beams failed in a brittle manner. It was observed that the lattice unit beam's initial fracture occurred at smaller displacements and the magnitude of maximum bending load was lower when compared to the solid beam. Since, the 8×3 and 12×3 lattice beam had multiple connecting links due to which the early failure occurred followed by total failure in a disrupted fashion. Similar observations were also reported in the previous publication [16] where structures containing triangular and hexagonal lattices showed disruptive failures. Moreover, fracture pattern of the optimised lattice unit beams are shown in Figure 9. It was observed that the bottom horizontal link had the first point of failure, followed by the failure in the links as shown in Figure 9.

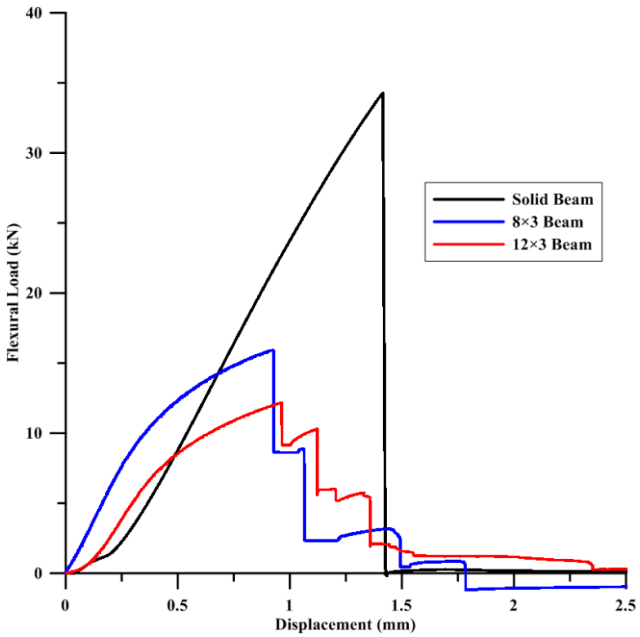

Figure 8. Load vs. displacement behaviour of the SLM-printed AlSi12 samples under bending load.

Table 2. Bending test results for solid and two TO beam types

Beam Type	Maximum Bending Load (kN)	Deflection at maximum bending load (mm)	Deflection at complete failure (mm)
Solid	31.45 ± 2.82	1.39 ± 0.03	1.39 ± 0.03
8×3	14.97 ± 0.83	0.89 ± 0.10	1.68 ± 0.11
12×3	11.03 ± 1.07	0.73 ± 0.16	1.84 ± 0.63

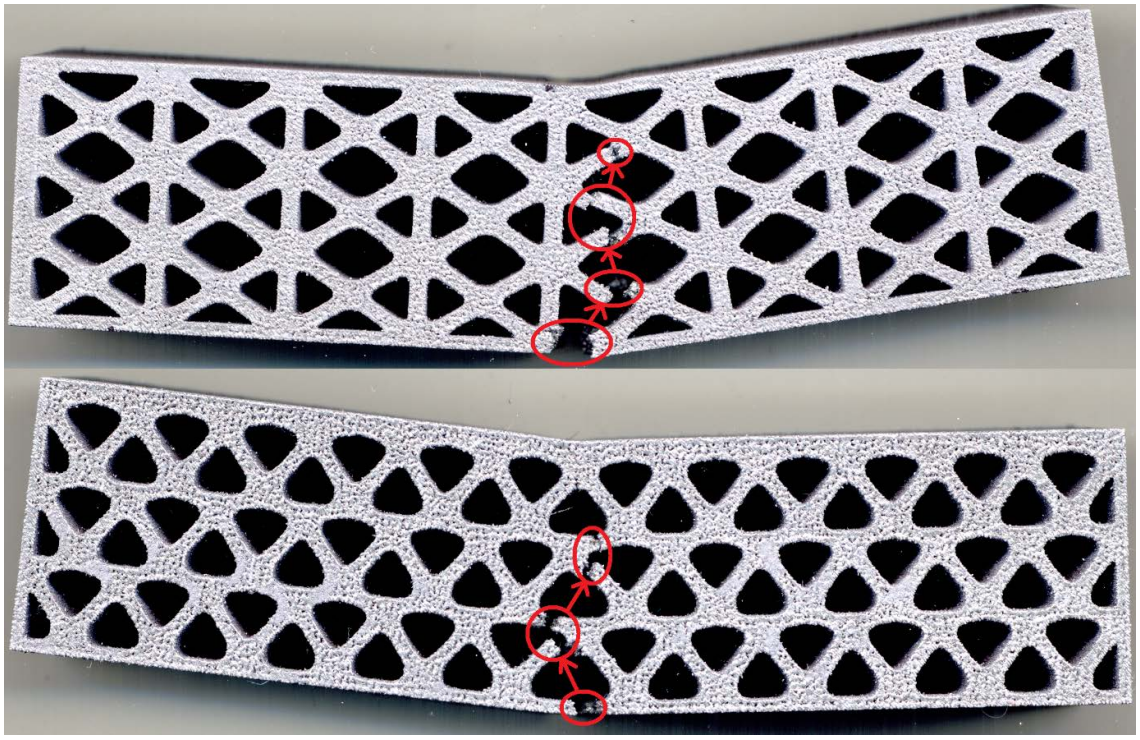

Figure 9. Failure pattern of the optimised lattice unit beams with direction of crack propogation; top – 8×3 lattice unit beam, bottom – 12×3 lattice unit beam.

Discussions

The performance of the beams in bending is evaluated by comparing energy absorbed per unit volume [2] during the flexural tests prior to complete failure. It was found that the total energy absorbed per unit volume by the BESO-optimised (TO) lattice unit beams were higher than that of the solid beam as shown in Figure 9. Also, the energy absorbed per unit volume till maximum load of 8×3 beams were superior than that of solid and 12×3 beams. This indicates that the optimised beams with adequate periodicity of lattice units performs better than the solid beam in energy absorbing applications. Similarly, lattice units with excellent energy absorbing ability were observed by du Plessis et. al. [22] in a recent publication. Further, the reason for the higher energy absorption is that fracture occurs in links along the loading direction one after another. This allows sufficient energy absorption by links prior to complete failure. But in the case of solid beam, initial crack in the beam causes instantaneous failure. It was also found that the BESO lattice unit beams reached maximum bending loads at very small displacement when compared to the solid beam. This implies that the application of BESO lattice units printed using SLM, in this case, could be restricted to applications where the deflection is not higher than 0.7 mm. Also, these attributes are generally related to structural members designed using lattice units.

The performance of the beams was also compared with the help of ratio of energy absorbed per unit volume at the point of maximum bending load (i.e. where the fracture

[2]Energy absorbed per unit volume by the beam is the ratio of the area under the force vs displacement plot to the material volume of the beam under consideration.

occurred). ‘Rs’ is the ratio of average energy absorbed per unit volume by BESO lattice unit beam till the deflection at maximum bending load to average energy absorbed per unit volume by the solid beam at the same deflection. The ratio is calculated and tabulated in Table 3 for 8×3 and 12×3 beams. It could be concluded that the BESO lattice unit beams could absorb more energy per unit volume i.e. around seven times, when compare to energy absorbed per unit by the solid beam.

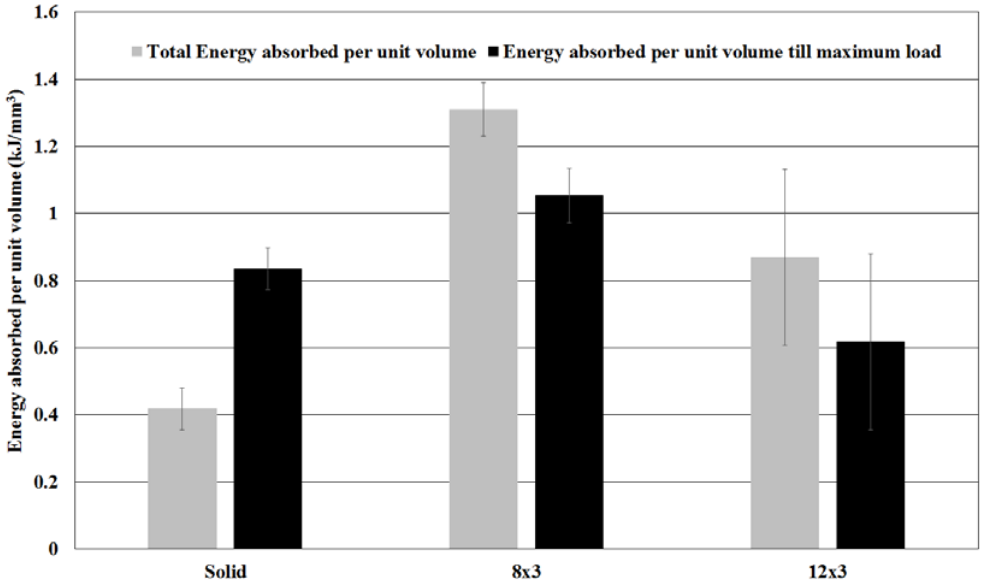

Figure 10. Comparison of the total energy absorbed per unit volume and energy absorbed per unit volume till maximum load by three different beams.

Table 3. Ratio ‘Rs’ calculated for beam 8×3 and 12×3

BESO lattice unit beam	Deflection at Maximum load (mm)	Energy absorbed per unit volume at this deflection (kJ/mm³)		Rs
		BESO lattice unit beam	Solid	
8×3	0.89 ± 0.10	1.05 ± 0.07	0.14 ± 0.05	7.50
12×3	0.73 ± 0.16	0.62 ± 0.16	0.09 ± 0.06	6.90

The BESO lattice unit beams considered for this study, i.e. 8×3 and 12×3 beams, showed similar bending behaviour as reported in [16]. The SLM-printed lattice unit beams failed in steps along the loading plane. The total energy absorbed per unit volume for complete failure for the two BESO-optimised beams was higher than the solid counterpart. However, the 12×3 beam type showed reduced maximum bending load caused by early failure. This could be due to the presence of variable cross-section along the plane of bending load, which resulted in stress concentration. However, in the case of the 8×3 beam, there is vertical link along the plane of bending load, which provides resistance to bending load, resulting in higher maximum

bending loads. Therefore, based on the application, periodicity of the lattice units could be varied to suit the loads applied.

Conclusion

A study was carried out to obtain an optimised design solution of a bending beam with the help of topology optimised lattice units. The samples were printed using Selective Laser Melting (SLM) process and a comparison of the flexural properties of solid beam to topology optimised lattice unit beams was made. Some key findings of the study are as follows.

- An ABAQUS subroutine was used for topology optimisation of a beam with BESO optimised lattice unit.
- Two unique lattice units (namely 8×3 lattice unit and 12×3 lattice unit) were obtained using the subroutine.
- The BESO lattice unit beams were found to absorb more energy per volume till complete failure when compared to solid beam.
- The BESO lattice unit beams also showed about seven times more energy absorption per unit volume at the same deflection of solid beam till the maximum load.

Importantly, the performance of BESO lattice unit beams were hampered by the brittle failure of SLM-printed parts. With improvement in the ductility of metal additive manufactured parts, the BESO lattice units could sustain higher bending loads. This opens up an avenue to reduce the weight of components by replacing solid material with tailored and topologically optimised lattice unit units depending upon the requirements of the application.

References

1. Sigmund, O. and Maute, K., *Topology optimization approaches.* Structural and Multidisciplinary Optimization, 2013. **48**(6): p. 1031-1055.
2. Aremu, A., Ashcroft, I., Hague, R., Wildman, R., and Tuck, C. *Suitability of SIMP and BESO topology optimization algorithms for additive manufacture*. in *21st Annual International Solid Freeform Fabrication Symposium - An Additive Manufacturing Conference, SFF 2010*. 2010.
3. Sigmund, O., *A 99 line topology optimization code written in matlab.* Structural and Multidisciplinary Optimization, 2001. **21**(2): p. 120-127.
4. *Tosca*. 2017 [cited 2017 23-02-2017]; Available from: https://www.3ds.com/products-services/simulia/products/tosca/.
5. *GENESIS Structural Optimization Extension for ANSYS Mechanical*. 2017 [cited 2017 19-06-2018]; Available from: http://www.vrand.com/products/gsam-gtam/.
6. *Easy to Use Optimization, Analysis, & Simulation Software | solidThinking Inspire*. 2017 [cited 2017 23-02-2017]; Available from: http://www.altairhyperworks.com/product/solidthinking-inspire.
7. Huang, X., *Evolutionary topology optimization of continuum structures : methods and applications*, ed. Y.M. Xie and I. Wiley. 2010, Chichester, West Sussex: Chichester, West Sussex : Wiley.
8. Xiao, Z., Yang, Y., Xiao, R., Bai, Y., Song, C., and Wang, D., *Evaluation of topology-optimized lattice structures manufactured via selective laser melting.* Materials & Design, 2018. **143**: p. 27-37.

9. Zhang, B., Pei, X., Zhou, C., Fan, Y., Jiang, Q., Ronca, A., D'Amora, U., Chen, Y., Li, H., Sun, Y., and Zhang, X., *The biomimetic design and 3D printing of customized mechanical properties porous Ti6Al4V scaffold for load-bearing bone reconstruction.* Materials & Design, 2018. **152**: p. 30-39.
10. García-Moreno, F., *Commercial Applications of Metal Foams: Their Properties and Production.* Materials, 2016. **9**(2): p. 85.
11. Rezaie, R., Badrossamay, M., Ghaei, A., and Moosavi, H. *Topology optimization for fused deposition modeling process*. in *Procedia CIRP*. 2013.
12. Castilho, M., Dias, M., Gbureck, U., Groll, J., Fernandes, P., Pires, I., Gouveia, B., Rodrigues, J., and Vorndran, E., *Fabrication of computationally designed scaffolds by low temperature 3D printing.* Biofabrication, 2013. **5**(3).
13. Gardan, N., *Knowledge Management for Topological Optimization Integration in Additive Manufacturing.* International Journal of Manufacturing Engineering, 2014. **2014**: p. 9.
14. Brandt, M., Sun, S., Leary, M., Feih, S., Elambasseril, J., and Liu, Q., *High-value SLM aerospace components: From design to manufacture*, in *Advanced Materials Research*. 2013. p. 135-147.
15. Okunkova, A., Volosova, M., Peretyagin, P., Vladimirov, Y., Zhirnov, I., and Gusarov, A.V., *Experimental Approbation of Selective Laser Melting of Powders by the Use of Non-Gaussian Power Density Distributions.* Physics Procedia, 2014. **56**: p. 48-57.
16. Rahman Rashid, R.A., Mallavarapu, J., Palanisamy, S., and Masood, S.H., *A comparative study of flexural properties of additively manufactured aluminium lattice structures.* Materials Today: Proceedings, 2017. **4**(8): p. 8597-8604.
17. Huang, X. and Xie, Y.M., *Convergent and mesh-independent solutions for the bi-directional evolutionary structural optimization method.* Finite Elements in Analysis and Design, 2007. **43**(14): p. 1039-1049.
18. Huang, X. and Xie, Y.M., *Optimal design of periodic structures using evolutionary topology optimization.* Structural and Multidisciplinary Optimization, 2008. **36**(6): p. 597-606.
19. Da, D., Xia, L., Li, G., and Huang, X., *Evolutionary topology optimization of continuum structures with smooth boundary representation.* Structural and Multidisciplinary Optimization, 2018. **57**(6): p. 2143-2159.
20. Rashid, R., Masood, S.H., Ruan, D., Palanisamy, S., Rahman Rashid, R.A., Elambasseril, J., and Brandt, M., *Effect of energy per layer on the anisotropy of selective laser melted AlSi12 aluminium alloy.* Additive Manufacturing, 2018. **22**: p. 426-439.
21. Ziółkowski, G., Chlebus, E., Szymczyk, P., and Kurzac, J., *Application of X-ray CT method for discontinuity and porosity detection in 316L stainless steel parts produced with SLM technology.* Archives of Civil and Mechanical Engineering, 2014. **14**(4): p. 608-614.
22. du Plessis, A., Broeckhoven, C., Yadroitsev, I., Yadroitsava, I., and le Roux, S.G., *Analyzing nature's protective design: The glyptodont body armor.* Journal of the Mechanical Behavior of Biomedical Materials, 2018. **82**: p. 218-223.